CHAPTER – 2

SYNTHESIS, CHARACTERIZATIONS AND ANALYSIS TECHNIQUES

2.1 Overview

This chapter describes sample processing method and the experimental techniques, utilized in its characterisation. In the present investigations, samples were prepared by solid state reaction route and solution based auto-combustion routes. Prepared compositions were characterized for their structural, micro-structural, thermal and photo physical properties.

2.2 Synthesis and processing of the compositions

For synthesis of various compositions, high purity raw materials were used. The specifications of these materials are listed in Table 2.1.

Table 2.1: Specifications of the materials used.

S.N.	Raw Materials	Chemical Formula	Purity (%)	Manufacturer
1.	Yttrium Oxide	Y_2O_3	99.99	Alfa Aesar
2.	Titanium Oxide	TiO_2	99.9	Alfa Aesar
3.	Erbium Oxide	Er_2O_3	99.98	Alfa Aesar
4.	Ytterbium Oxide	Yb_2O_3	99.99	Alfa Aesar
5.	Lithium Carbonate	Li_2CO_3	99.98	Merck
6.	Calcium Carbonate	$CaCO_3$	99.99	Sigma Aldrich
7.	Europium Oxide	Eu_2O_3	99.5	Alfa Aesar
8.	Gadolinium Oxide	Gd_2O_3	99.99	Alfa Aesar
9.	Ammonium Molybdate	$(NH_4)_6Mo_7O_{24}\cdot 4H_2O$	99.0	Alfa Aesar
10.	Urea	NH_2CoNH_2	98.0	Sigma Aldrich

A few other high grade chemicals, solvents and reagents like Acetone, Nitric acid, Hydrochloric acid, polyvinyl Alcohols, ethylene glycol, urea, ammonia solution etc. were also utilized to synthesize the samples.

2.2.1 Synthesis routes

In order to process the materials two, different syntheses routes viz. solid state ceramic route and auto-combustion were adopted.

2.2.1.1 Solid state reaction route

Samples were prepared by a conventional solid-state ceramic method. Analytical reagent (AR) grade different ingredients were used as the starting materials. Stoichiometric amounts of these materials were mixed in a planetary ball mill with zirconia jars and zirconia balls for 6h at 50 rpm using acetone as the mixing medium(solvent).The dried mixed powders were calcined in an alumina crucible in an ambient atmosphere (air) at1200 ^{o}C for 6h, and then the samples were furnace cooled to room temperature. A few drops of a 2% solution of polyvinyl alcohol (PVA) were added to the powder as the binder. The calcined powders were ground, mixed, and pelletized at 75 kN. The pellets were sintered at1300 ^{o}C for 12h. During sintering, the pellets were initially heated at a rate of 2 ^{o}C per min to 500 ^{o}C and then kept at this temperature for 1 h to evaporate the binder. Then, the pellets were heated at a rate of 4 ^{o}C per min to the sintering temperature of 1300 ^{o}C. After sintering, the samples were furnace cooled to room temperature.

A detailed procedure of the solid state reaction route is shown in schematic block diagram of Figure 2.1.

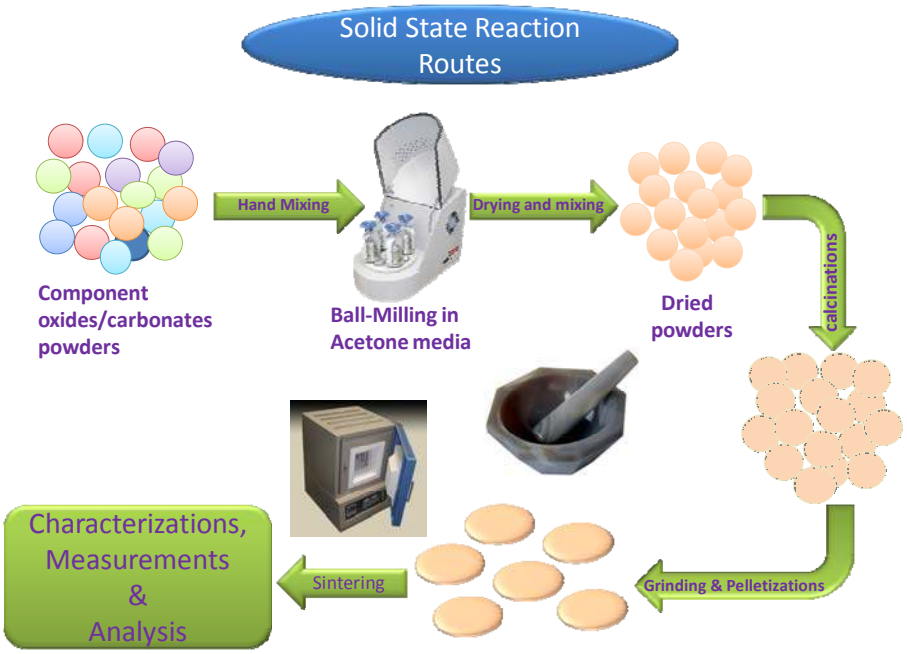

Figure 2.1: Schematics of Solid state reaction route.

2.2.1.2 Chemical routes

It is well known fact that performance of materials rely on synthesis routes by which it is processed (Kong et al, 2008). Synthesis methodology of the synthesized materials has a prominent role in determining the microstructure, photoluminescence properties, and quantum efficiency of the phosphor.

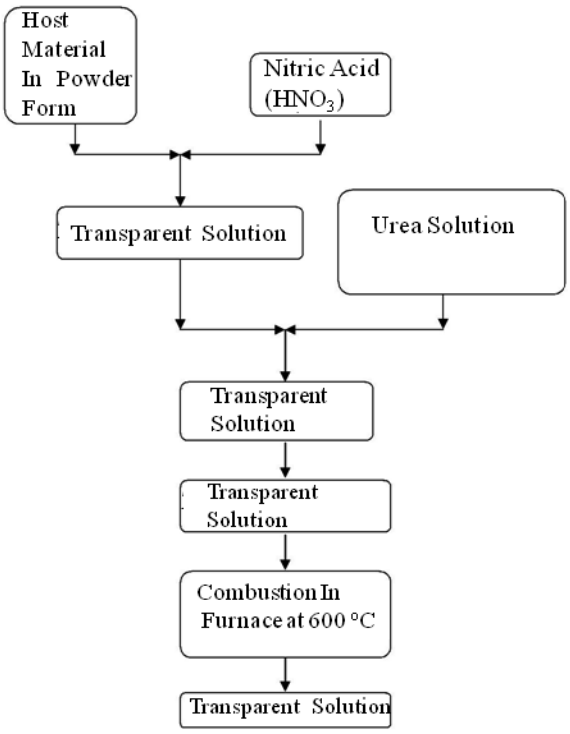

Figure 2.2: Schematic representation of facile auto-combustion technique.

Solution combustion synthesis route has been proven as excellent technique as one has wide range of flexibility in the selection of fuels and a rapid cooling process which hinders the nucleation growth of the crystallites, enabling non-agglomerated nanocrystals of high purity with nano-size. The Schematic representation of facile auto-combustion technique has been shown in Figure 2.2. This methodology makes it possible to prepare nonmaterial with versatile compositions of different concentrations which is easily doped with various ions. The method utilizes the energy produced by the exothermic decomposition of a redox mixture of metal nitrates with an organic fuel (e.g. urea, carbohydrazide, or glycine). During the combustion, exothermic redox reactions associated with nitrate decomposition and fuel oxidation take place. For the reaction to

take place, large amount of heat energy is necessary during the formation of the final compound. For example, when Al_2O_3 is desired to be prepared through a reaction of $Al(NO_3)_3$ and urea (NH_2CONH_2),the enthalpy of the reaction is seen to be negative of the order of 2700 KJ/mol.

$$2Al(NO_3)_3 * 9H_2O + 5\ NH_2CONH_2 \rightarrow \ Al_2O_3 + 5CO_2 + 28H_2O + 8N_2\uparrow + \Delta H$$

where $\Delta H \sim -2700$ kJ/mol

In the first step of the decomposition, cyanuric acid is formed at temperatures between 120 – 250 ^oC. At a later stage at temperatures between 300 – 450 ^oC depolymerization of cyanuric acid occurs. Biuret is a condensation product of urea. The decomposition process is indicated below:

$$NH_2CONH_2 \rightarrow HNCO + NH_3 \qquad (130 – 250\ ^oC)$$

$$NH_2CONH_2 + HNCO \rightarrow NH_2CONHCONH_2 \qquad (190 – 250\ ^oC)$$

$$HNCO + H_2O \rightarrow CO_2 + NH_3 \qquad (300 – 450\ ^oC)$$

A stoichiometric mixture of metal nitrates and the appropriate amount of fuel are mixed such that it can react completely with all the metal nitrates in the mixture, and no residual fuel or nitrate remains in the product material. The gases such as N_2, CO_2, H_2O are the end products under complete combustion. Stoichiometry of a metal nitrate and fuel mixture is determined by stoichiometric coefficient, φ [Jain, et al. (1981)].

$$\Phi = \frac{\sum(\text{Coefficient of oxidizing elements in a specific formula x (valency)})}{(-1)\sum(\text{Coefficient of reducing elements in a specific formula x (valency)})}$$

The coefficients for the oxidizing and reducing elements are obtained from the balanced chemical equation of metal nitrates and fuel involved in the combustion process. Depending upon the value of Φ, these mixtures are distinguished as:

$\Phi = 1$; mixture is stoichiometric

$\Phi > 1$; mixture is fuel deficient

$\Phi < 1$; mixture is fuel rich

The stoichiometric coefficient requires a calculation of the oxidizing and reducing valences. The oxidizing element with positive value is oxygen and reducing elements with negative values are carbon, hydrogen and metal (e. g. Al in Al $(NO_3)_3$) are reducing elements. Nitrogen is considered to be neutral (zero valence). For example, for $Ca(NO_3)_2$, Ca yields a value of 2[1*(+2) = 2], N has a zero valence, while oxygen contributes – 12 [2*3(-2)] with a total valence of -10. On the other hand for the reducing agent, NH_2CONH_2 i.e. urea, N contributes 0, H and C +4 each, while O contributes -2 making a total of +6. With these values it is easy to see that for a mixture of $Ca(NO_3)_2$ and NH_2CONH_2 the stoichiometric ratio is 10:6 or 1.667, or we need to mix one mol of calcium nitrate and 1.667 mol of urea.

The mechanism of the combustion reactions is somewhat complex because several intermediate reactions are also involved. The driving force for the self-propagating reaction is the enthalpy of the exothermic reaction, and it is necessary that the local rate of heat generation from the exothermic chemical reaction is large enough to meet the various rates of heat redistribution needed to initiate the reaction of the precursor materials. The factors restricting forward propagation of the reaction are the endothermic reactions which form the intermediate complexes, and the heat of vaporization of reactants, and include heat loss through conduction, convection or radiation. The heating rate of precursor solution, stoichiometry, the container used, and the environment all influences the process of combustion [Kingsley, et al. (1988)]. Mass to volume ratio of the reactants is a very important factor because it controls the temperature. This is illustrated by the fact that reaction of 5g of mixed aluminium nitrate and urea kept in a container of 500 ml capacity (100 mm diameter and 50 mm height) does not ignite, but ignition occurs when the same amount is placed in a smaller 100 ml capacity (50 mm diameter and 20 mm height) container.

2.3 Characterizations techniques

Following characterization and analysis techniques have been employed to investigate the samples in the present thesis.

2.3.1 Differential Thermal Analysis (DTA) and Thermo Gravimetric Analysis (TGA)

Differential thermal analysis (DTA) is a technique which involves heating or cooling of a test sample and an inert reference sample under identical conditions. In this method temperature difference which develops between test and reference sample are recorded. In this method, the fine powder material under investigation is placed in a small capsule, often of alumina or other suitable refractory material. A second identical capsule containing an inert powder such as α-Al_2O_3, which does not exhibit endothermic or exothermic effects, is placed adjacent to the test sample. Thermocouples are embedded in the test substance and in the α-Al_2O_3 powder and are connected, so that their e.m.f.s is opposed. The resultant e.m.f therefore corroborates the temperature difference between the sample powder and the inert α-Al_2O_3.

The two capsules are heated at a constant rate and the temperature difference is plotted either against time or against the temperature at some fixed points. Any physical or chemical change occurring in the test sample involves the evolution of heat, will cause its temperature to rise temporarily above that of reference sample leading to an exothermic peak. Conversely, a process, which is accompanied by the absorption of heat, will cause the temperature of the test sample to lag behind that of the reference sample, leading to an endothermic peak. The area under any given peak can be used as a quantitative measure of the amount of heat evolved or absorbed by the physical or chemical changes, which had occurred.

Thermo gravimetric analysis (TGA) is a technique for measuring the change in weight of a substance as a function of temperature. The sample (usually a few milligrams in weight) is heated at a constant rate, typical in the range 1 to 20 °C min^{-1} and has a constant weight until it begins to decompose at a certain temperature. Under dynamic heating decomposition occurs over a range of temperature and after certain temperature no weight loss is observed leading to the completion of decomposition reaction. The weight losses are fundamental properties of the sample and can be used for quantitative calculations of compositional changes involved.

To know the temperature at which completion of reaction occurred and no significant weight loss observed, differential thermal analysis (DTA) and thermo

gravimetric analysis (TGA) were carried out simultaneously on the collected gel samples (prior to ignition) employing the instrument Diamond TGA/DTA Perkin Elmer, USA at a heating rate of 10 °C / min. upto 1000 °C in air.

2.3.2 Phase Formation and Crystal Structure Studies by Powder X-Ray diffraction

X-ray diffraction (XRD) is a versatile, non-destructive technique that reveals detailed information about crystallographic structure of materials. X-ray radiations most commonly used, are copper K_α radiation with wavelength =1.5406Å. When the X-ray radiation strikes a powder sample, diffraction occurs in every possible orientation of 2θ. The X-ray radiation strikes with all possible orientations of all possible lattice planes present in a powder sample. Hence, one can easily record the diffraction peaks corresponding to different crystal planes. Analysis of data is carried out by comparing the diffractogram obtained from the powder with an internationally recognized database containing reference patterns of various samples. The diffracted beam is detected by using a movable detector such as a Geiger counter, which is connected to a chart recorder. In normal use, the counter is set to scan over a range of 2θ values at a constant angular velocity. Generally, a 2θ range of 10 to 90 degrees is sufficient to cover the most useful part of the powder diffraction pattern. Crystals are composed of regularly spaced atoms which can act as the scattering centres for X-rays and the X-rays are electromagnetic waves of wavelength (0.5-2.5 Å) which is equivalent to the inter-atomic distance in crystals. In this condition the X-rays suffers diffraction by the crystals. W. L. Bragg gave the conditions for the X-ray diffraction from the crystals, known as Bragg's law. When a monochromatic X-ray beam of wavelength λ is incident on a perfect crystal at an angle Θ, having interplaner spacing d, diffraction maxima occurs only when the path difference between the rays reflected from the successive planes is integral multiple of λ.

Bragg's law can be expressed as

$$(2d \sin\theta = n\lambda; \text{ where } n= 1, 2, ...) \qquad (2.1)$$

where n is known as the order of reflection. For fixed λ, different sets of θ and d satisfy the Bragg's conditions to give the diffraction maxima. The scanning speed of the counter is usually 2θ (~ 2degrees min^{-1}). A host of application techniques for various material classes are available, each revealing its own specific details of the sample studied.

The single or multiple phases confirmation in an unknown sample is the main implication of X-ray powder diffractometry. Phase identification enables us to understand the formation of these samples.

To check the single phase formation, powder X-ray diffraction was done at different stages (i.e. as burnt ash, calcined and sintered) of synthesis. The powder of as burnt ash, calcined and sintered pellets was ground and powder X-ray diffraction patterns were recorded using an X-ray Diffractrometer (Rigaku Miniflex II) employing Cu-Kα radiation with Ni filter. The formation of single-phase solid solution was confirmed by the absence of characteristic lines of the constituent oxides. The XRD patterns were indexed with the help of the standard charts available in literature. The lattice parameters were determined using non-linear least square fitting of the data using a software program 'UnitCell'. The crystallite size was estimated by X-ray line broadening analysis.

It has been assumed that a perfect crystal that would extend in all directions to infinity, so one can say that no crystal is perfect due to its finite size. The effect of this deviation from perfect crystallinity leads to the broadening of a diffraction peak. However, above a certain size (100-500 nm), this type of broadening is negligible. It was observed that small crystallite size could give rise to line broadening. A well-known equation relating the crystallite size to the line broadening, which is called 'Debye-Scherrer Formula and mathematically given as:

$$D = \frac{0.9\lambda}{\beta \cos\theta} \qquad (2.2)$$

D is the average crystallite size, λ is the wavelength of the X-rays (1.5406Å), and θ and β are the diffraction angle and full-width at half maximum (FWHM) of the peak in the XRD pattern, respectively. For β correction, β_{inst} (*FWHM* due to instrument) is removed using *Si* standard. It is termed as average crystallite size because the X-rays beam irradiates a large number of crystallites so that the value of d obtained represents the mean value of the actual size distribution.

In order to understand the structural analogue and cite symmetry variation to influence the luminescence properties, their structural information has to be known more precisely. R.M. Rietveld has firstly developed a structure profile refinement method for powder diffraction data of X-ray and Neutron radiations. Rietveld refinement method creates an effective separation of these overlapping data, thereby allowing an accurate

determination of structure. In the Rietveld refinement the least square refinement is carried out until the best fit is obtained between the entire observed powder diffraction patterns taken as a hole and entire calculated pattern based on simultaneously refined model for crystal structure. Therefore applying the Rietveld refinement method to a powder diffraction pattern, it is possible to obtain much more information about the structure factors of the material.

The shape of a powder diffraction reflection is influenced by the characteristics of the beam, the experimental arrangement, and the sample size and shape. In the case of monochromatic neutron source the convolution of the various effects has been found to result in a Gaussian shape. If the distribution is assumed to be Gaussian, then the contribution of a given reflection to the profile y_i at position $2\theta_i$ is:

$$y_i = I_k \exp\left[\frac{-4\ln(2)}{H_k^2}\left(2\theta_i^2 - 2\theta_k^2\right)\right] \tag{2.3}$$

where H_k is the full width at half peak height (full-width half-maximum), $2\theta_k$ is the centre of the reflex, and I_k is the calculated intensity of the reflex (determined from the structure factor, the Lorentz factor, and multiplicity of the reflection). At very low diffraction angles the reflections may acquire an asymmetry due to the vertical divergence of the beam. Rietveld used a semi-empirical correction factor, A_s to account for this asymmetry:

$$A_s = 1 - \left[\frac{sP\left(2\theta_i - 2\theta_k\right)^2}{\tan\theta_k}\right] \tag{2.4}$$

The width of the diffraction peaks are found to broaden at higher Bragg angles. This angular dependency was originally represented by

$$H_k^2 = U\tan^2\theta_k + W \tag{2.5}$$

where U, V and W are the half width parameters and may be refined during the fit. The principle of the Rietveld Method is to minimize a function M which analyzes the difference between a calculated profile y_{calc} and the observed data y_{obs}. The function M is derived as:

$$M = \sum_i W_i \left\{ y_i^{cal} - \frac{1}{c} y_i^{obs} \right\}^2 \tag{2.6}$$

where W_i is the statistical weight and c is an overall scale factor such that $y^{cal} = y^{obs}$. In present thesis, Rietveld refinement has been performed using *FullProf* software.

2.3.3 X-ray Photoelectron Spectroscopy

X-ray photoelectron spectroscopy (XPS) is a surface-sensitive quantitative spectroscopic technique that measures the elemental composition at the parts per thousand range, empirical formula, chemical state and electronic state of the elements that exist within the material. XPS spectra are obtained by irradiating a material with a beam of X-rays while simultaneously measuring the kinetic energy and number of electrons that escape from the top 0 to 10 nm of the material being analyzed. XPS requires ultra-high vacuum (UHV; $P < 10^{-9}$ millibar) conditions, although a current area of development is ambient-pressure XPS, in which samples are analyzed at pressures of a few tens of millibar. XPS is a non-destructive surface chemical analysis technique that can be used to analyze the surface chemistry of a material in its as-received state, or after some treatment, for example: fracturing, cutting or scraping in air or UHV to expose the bulk chemistry, ion beam etching to clean off some or all of the surface contamination (with mild ion etching) or to intentionally expose deeper layers of the sample (with more extensive ion etching) in depth-profiling XPS, exposure to heat to study the changes due to heating, exposure to reactive gases or solutions, exposure to ion beam implant, exposure to ultraviolet light.

2.3.4 Transmission Electron Microscopy (TEM)

In this technique a beam of electron is allowed to transmit through an ultrafine thin sample, interacting with it. An image of the particles of the sample is formed from the interaction of the electrons transmitted through the sample, which is magnified and focused onto an imaging device, such as a fluorescent screen, as is common in most TEMs, on a layer of photographic film or detected by a sensor such as a CCD camera. TEM is capable of imaging at a significantly higher resolution because of the small de Broglie wavelength of electron. This enables the instrument to be able to examine fine details even as small as a single column of atoms. At low magnification TEM image contrast is due to absorption of electrons in the sample, due to the thickness and composition of the sample. At high magnification complex wave interactions modulate the intensity of the image, requiring an expertise analysis of observed image. This technique is used to observe modulation in chemical identity, crystal orientation, electronic structure and sample induced electron phase shift as well as the regular absorption based imaging.

The most common mode of operation for TEM is the bright field imaging mode. In this mode the contrast is due to occlusion and absorption of electrons in the sample

(classically). Thicker regions of the sample or region with higher atomic number will appear dark, whilst regions with no sample in the beam path will appear bright (hence the term bright field).

High-resolution transmission electron microscopy (HRTEM) is another imaging mode of the transmission electron microscope that allows the imaging of the crystallographic structure of a sample at an atomic scale. Because of its capacity to give very high resolution, it is an invaluable tool to study nano-scale properties of crystalline materials. In contrast to conventional microscopy, HRTEM does not use amplitudes, i.e. absorption by sample, for image formation. Instead, contrast arises from the interference in the image planes of the electron waves itself. Due to our inability to record the phase of these waves, we generally measure the amplitude resulting from this interference, however the phase of the electron wave still carries the information about the sample and generates contrast in the image, thus name phase-contrast imaging. However, this is true only if the sample is thin enough so that amplitude affects the image only slightly.

Selected area electron diffraction (SAED or SADP) is a crystallographic experimental technique that can be performed inside a transmission electron microscope. In this case, electrons are treated as wave like rather than particle. Since the wavelength of high energy electron is a fraction of a nano-meter and the spacing between atoms in a solid is only slightly larger, the atoms act as a diffraction grating to the electron, which are diffracted. As a result, the image on the screen of the TEM will be a series of spots (selected area diffraction pattern, SADP) and each spot correspond to follow Bragg's diffraction condition of the sample's crystal structure. If the sample is tilted, the same crystal will stay under illumination but different diffraction conditions will be satisfied and different diffraction spots will appear or disappear. For thin crystalline samples, this produces an image that consists of a series of dots in the case of a single crystal, or a series of rings in the case of a polycrystalline sample. For the single crystal case, the diffraction pattern is dependent upon the orientation of the sample. This image provides information about the space group, symmetries in the crystal and the crystal's orientation to the beam path.

To examine morphology of the as-prepared ash and calcined powder of a sample, transmission electron microscopy has been done using TECNAI 20 G^2 operated at an accelerated voltage of 200 kV and JEM-2100F, JEOL, Japan. The suspension of the particles was obtained and thereafter small amount of suspension were poured on copper grid (50 micron thick) and dried for an hour. The sample was then mounted on sample

holder and transferred to the TEM column. Morphology and the crystal structure were investigated by using real space imaging that is in bright field TEM mode and reciprocal space imaging by selected area electron diffraction patterns. High resolution transmission electron microscopy (HRTEM) has also been done on few samples.

2.3.5 Micro-structural Studies by Field Emission Scanning Electron Microscopy (FESEM)

A field-emission cathode in the electron gun of a scanning electron microscope provides narrower probing beams at low as well as high electron energy, resulting in both improved spatial resolution and minimized sample charging and damage. Under vacuum, electrons generated by a Field Emission Source are accelerated in a field gradient. The beam passes through Electromagnetic Lenses, focusing onto the specimen. As result of this bombardment secondary electrons are emitted from the specimen. A detector catches these secondary electrons and an image of the sample surface is constructed by comparing the intensity of these secondary electrons to the scanning primary electron beam. Finally the image is displayed on a monitor. Mechanism of FESEM is shown in Figure 2.3.

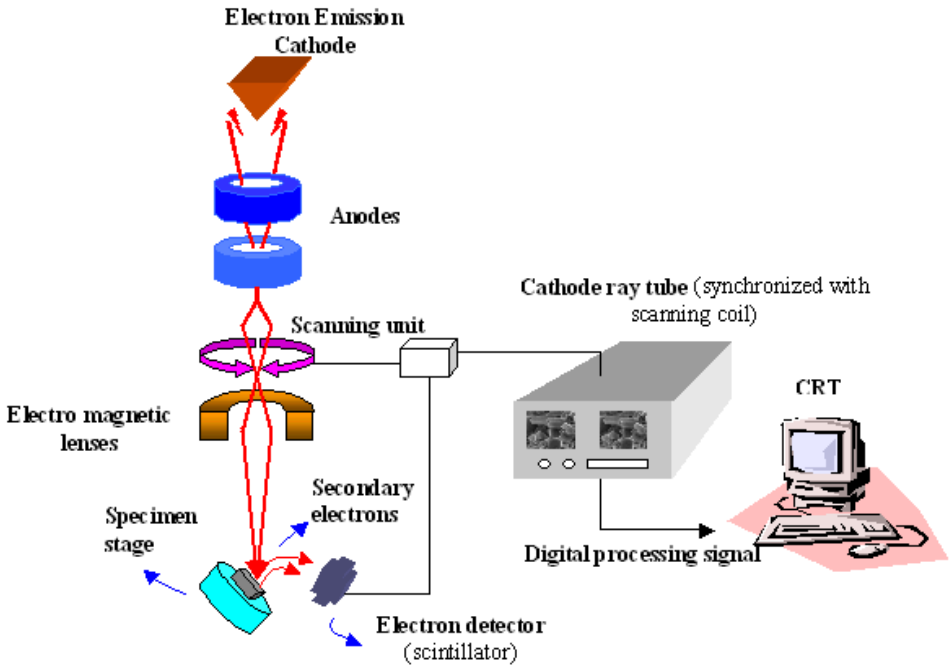

Figure 2.3: Mechanism of FESEM.

FESEM produces clearer, less electrostatically distorted images with spatial resolution down to 1-0.5 nm. It provides 3 to 6 times better resolution than conventional SEM. Smaller-area contamination spots can be examined at accelerating voltages

compatible with Energy Dispersive X-ray Spectroscopy. There is negligible electrical charging of samples and having high quality, low voltage images are obtained. The high-resolution accompanied by FESEM (~ 2 nm) allows the study of very small microstructural details, morphology analysis (particles shape and size), fracture studies, interface behavior, quantitative and qualitative elemental analysis. It can also be probed out for grain orientation, texture and phase identification of the sample.

The micrographs were recorded using Field Emission Scanning Electron Microscope (FESEM), JSM-6700, model JEOL, Japan.

2.3.6 Fourier Transform Infrared Spectrometer (FTIR)

Fourier transform infrared spectrometer has been used for measurement of infrared absorption bands of the compounds present in the sample. A simple block diagram of the FTIR spectrometer is shown in Figure 2.4. This instrument is similar to the Michelson inereferometer.

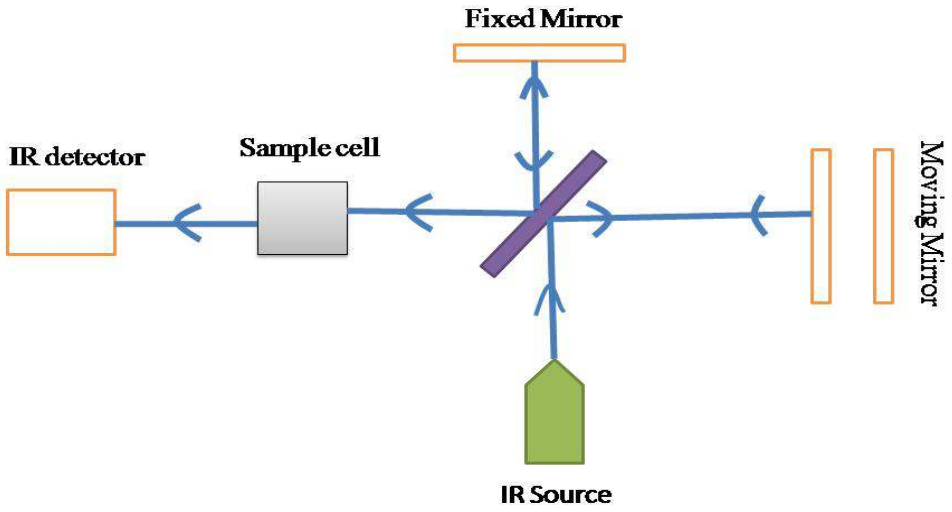

Figure 2.4: Block diagram of FTIR spectrometer.

Light from the IR source is splitted into two beams by KBr beam splitter. One beam goes towards fixed mirror and the other towards moving mirror. The moving mirror is used to introduce path difference between two beams. The beams reflected by two mirrors interfere at the beam splitter. The interference pattern for all infrared waves is observed simultaneously on the detector. Due to this interference a large number of sinusoidal waves appear at the detector. The moving mirror set a time delay between two interfering beams and converts the spectral information from the time domain to the space domain. On measuring the signals at different discrete positions, all the interfering frequencies

generates an interferogram, which is nothing but a large number of sinusoidal signals added to each other containing information about each IR wave amplitude, phase and wavelength. The time domain spectral information is converted into the frequency domain by Fourier transform of the measured signal. FTIR spectra have been recorded in the range of 400 – 4000 cm^{-1}.

2.3.7 Micro-Raman Analysis

The experimental set-up RM 1000 from Renishaw used consists of the following components:

(a) Ar^{+}-Laser of 50 mW

(b) Edge filter

(c) Microscope from Olympus with 50x long distance objective

(d) Grating as a dispersing elements

(e) Peltier cooled CCD Camera

(f) 514.5 nm line selector and plasma line filter for 514.5 nm line

The typical micro-Raman system consists of a microscope and an automated X-Y stage, excitation laser, filters, slit, diffraction grating, necessary optics, detector, and data-processing software. The micro-Raman set-up (Figure 2.5) consists of a microscope model MX 50 A/T from Olympus. The microscope was first operated in white light mode and focused image of the sample was seen on the computer screen. The microscope was then turned to laser mode to record the Raman spectra. The image can also be saved. The sample in the present case was kept in the sample holder of temperature cell, which creates a gap between the sample and the objective. Therefore long working distance plane achromatic objective of magnification 50X, numerical aperture 0.45, working distance 15 mm and resolution 0.75 μm was used.

Since the CCD is finite in size (there is spectral range and resolution of every CCD), which depends on the distance between the CCD and the grating apart from the intrinsic physical properties of the chips. Fluorescence sometimes causes problem with visible excitations, whereby weak bands are smeared out. But fortunately with the systems studied in this thesis, fluorescence was not a big problem.

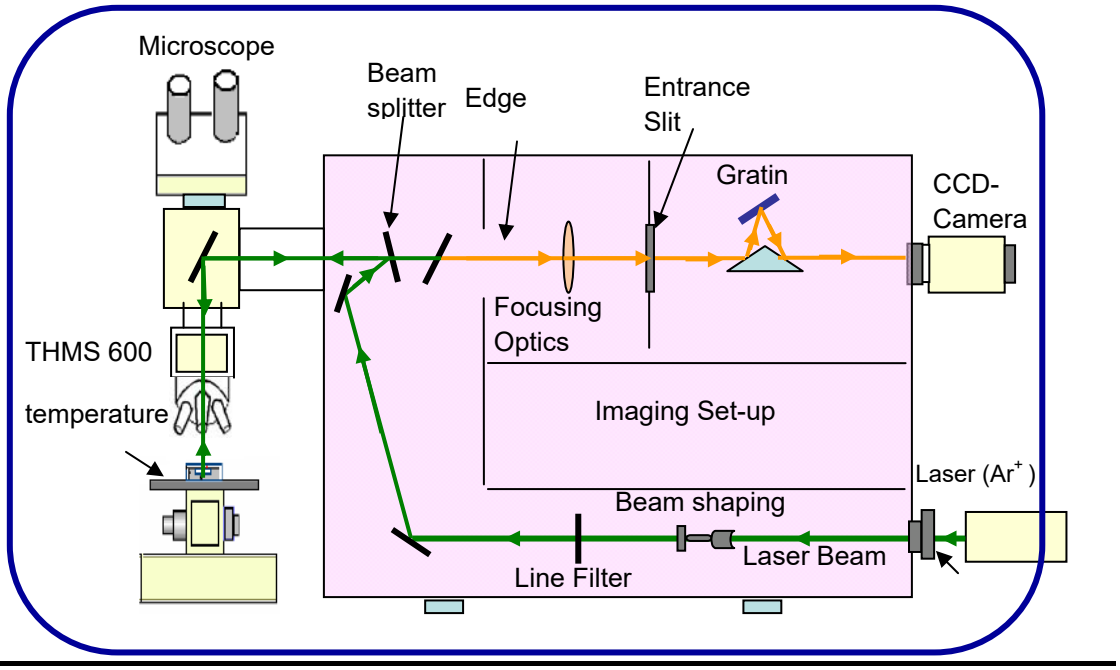

Figure 2.5: Micro-Raman set-up (Renishaw, Model RM 1000) with Ar^{+}-laser and heating cooling temperature cell THMS 600.

2.3.8 UV- Visible absorption measurement

A double beam UV-VIS spectrometer has been used to record the absorption spectrum in the range 200 – 1100 nm. The simple block diagram of the spectrometer is shown in Figure 2.6. Two light sources, a tungsten halogen lamp and a deuterium lamp, are used in most of the spectrometer to cover the given wavelength range. A lamp selection mechanism is present to select desired light source. In this case, radiation from continuous light source passes through a mono-chromator and resolved into its constituent wavelengths. A chopper is used to split the incoming light into two beams. One beam is passed through the reference sample and the other beam through the sample. The signals from the reference and the main sample are detected at photodiode 1 and 2, respectively. The difference amplifier is used to amplify the difference of signals detected by detector1 and 2. The obtained spectrum is displayed on the computer as a function of wavelength Vs absorbance. The intensity of sample and reference beam is defined as I and I_0. A ratio of I/I_0 is measured verses wavelength. The UV and visible scan is performed in the range 200-400 nm and having range from 400-800 nm, respectively. Absorption is expressed as: $A = \log_{10}\left(I_0 / I\right)$ (2.7)

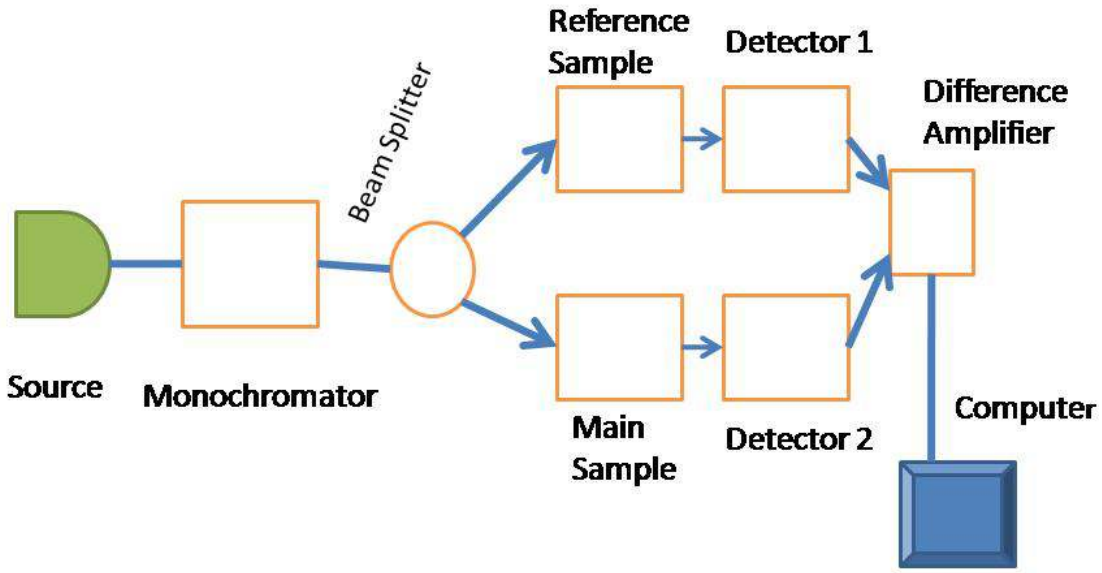

Figure 2.6: Block diagram showing the principle of UV-VIS spectrometer.

The wavelength corresponding to maximum absorbance is a characteristic value termed as λ_{max}. For highly absorbing compounds, absorption is performed in dilute solution. For these highly transparent solvents is required. The most commonly used solvents are namely water, ethanol, hexane and cyclohexane. One can generally avoid the use of solvents having double or triple bonds or heavy metals as S, Br and I. Since the absorbance of a sample is proportional to its molar concentration in the sample cuvette under consideration. In order to compare the different spectra of the compound, a corrected absorption value known as molar absorptivity is used. This is defined as Beer-Lambert law:

$$\text{Absorbance } A = \varepsilon c L \tag{2.8}$$

$$\text{Molar absorptivity, } \varepsilon = \frac{A}{cL} \tag{2.9}$$

Where c is sample concentration in mole/liter and L is the path length of the beam through the cuvette in centimetre.

2.3.9 Fluorescence and upconversion measurements

Systematic arrangements used for upconversion measurement is shown in Figure 2.7. The mono-chromator disperses the wavelength components present in the emitted fluorescence light. Photomultiplier tube converts optical signal corresponding to different wavelengths into electrical signal and amplify it. The Spectrometer and the excitation source used are given below:

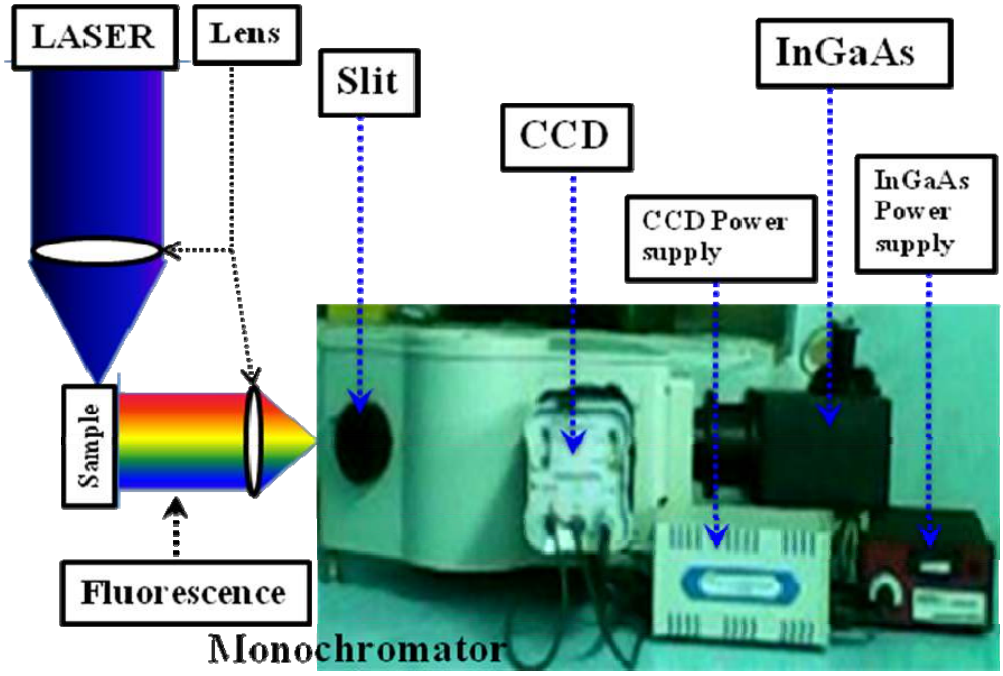

Figure 2.7: Experimental setup for recording steady state emission spectra.

2.3.9.1 Spectrometers

1. Spex 340E with S20 photomultiplier tube attached with chart scanning assembly.
2. Horiba Jobin Yuon computer controlled iHR320 m with R928P photon counting PMT (resolution ~ 0.6 nm) and
3. Ocean Optics QE65000 TE cooled CCD spectrometer has also been used in our measurements.

2.3.9.2 Lasers for excitation

(i) Nd^{3+}: YVO_4 C W laser (CW, 532 nm wavelength)

(ii) Nd^{3+}: YAG Pulsed laser (1064, 532, 355 and 266 nm wavelength,~7ns pulse width)

(iii) Diode laser (CW, 976nm wavelength)

2.3.9.3 Lifetime measurements

To measure the lifetime of the different levels involved in the radiative transition, the samples were excited either with CW diode laser by using a mechanical chopper or with pulsed Nd^{3+}: YAG laser to obtain intermittent irradiation. The monochromator was fixed at the wavelength of a particular transition. The decay profile was taken on an oscilloscope (~150MHz frequency, Hameg, Germany) attached with computer. Lifetime measurement setup is shown in Figure 2.8.

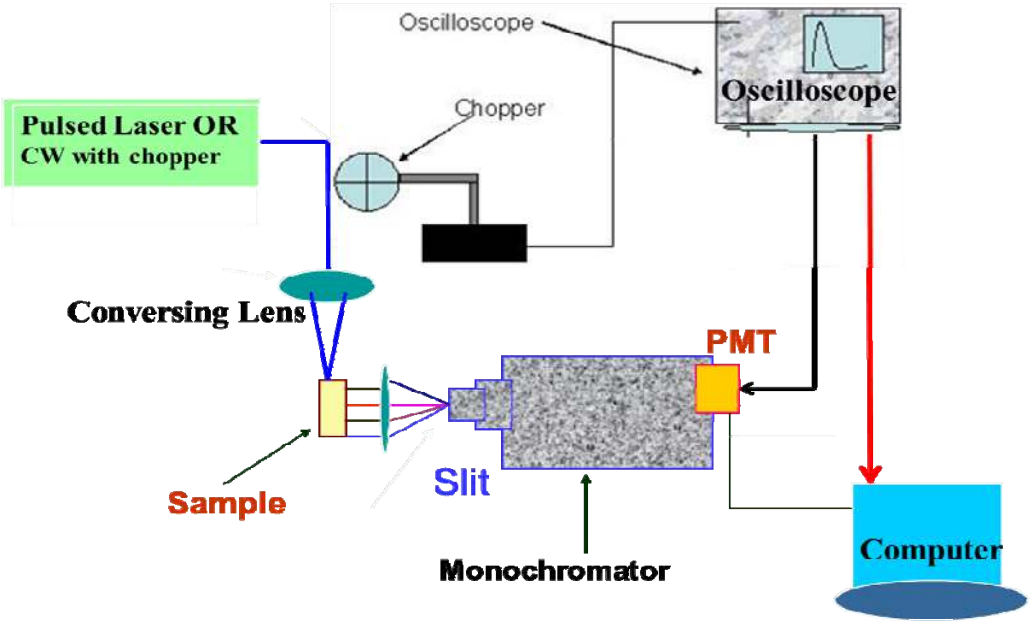

Figure 2.8: Experimental setup for lifetime measurements.

★★★★★★